Composite Structures 356 (2025) 118895

Contents lists available at ScienceDirect

Composite Structures

journal homepage: www.elsevier.com/locate/compstruct

Strength-based RSM optimization of concrete containing coarse recycled concrete aggregate and raw-crushed wind-turbine blade

Nerea Hurtado-Alonso [a], Javier Manso-Morato [b], Víctor Revilla-Cuesta [b,*], Marta Skaf [a]

[a] Department of Construction, Escuela Politécnica Superior, University of Burgos, c/ Villadiego s/n, 09001 Burgos, Spain
[b] Department of Civil Engineering, Escuela Politécnica Superior, University of Burgos, c/ Villadiego s/n, 09001 Burgos, Spain

ARTICLE INFO

Keywords:
Recycled concrete aggregate (RCA)
Raw-crushed wind-turbine blade (RCWTB)
Concrete
Optimization
Response surface method (RSM)
Mechanical strength

ABSTRACT

Recycled Concrete Aggregate (RCA) and Raw-Crushed Wind-Turbine Blade (RCWTB) are waste materials obtained from decommissioned wind turbines after crushing their foundations and blades, respectively. Their use as raw materials in concrete allows their recycling. RCA increases concrete sustainability, while the fibers of Glass Fiber-Reinforced Polymer (GFRP) in RCWTB (66.8 % wt.) improve its bending performance. Nevertheless, only balanced waste combinations provide an adequate concrete behavior. Following a characterization of concrete in terms of fresh and strength performance, Response Surface Method (RSM) was conducted based on the experimental results to define the optimum waste combinations to reach a concrete strength performance adequate for engineering applications. RSM highlighted the need to limit the RCWTB content to 3 % to reach a compressive strength higher than 45 MPa, while amounts below 3 % and above 7 % would allow obtaining a flexural strength over 5.5 MPa. In both cases, the maximum content of coarse RCA should be 80 %. 70 % coarse RCA and a RCWTB amount between 6 % and 10 % would enable to develop concrete mixes with conventional strengths of 30–40 MPa under compression and 5 MPa under bending. RSM results revealed that RCWTB and their GFRP fibers properly behave in concrete with coarse RCA.

1. Introduction

In recent years, the implementation of optimization tools in scientific research has become widespread, aimed at enhancing efficiency and facilitating accelerated advancements in various fields. Given that time, cost, and human resources are fundamental factors on which research relies, the application of these optimization tools is essential for maximizing results in their respective domains. In the field of the strength behavior of materials, reference can be made firstly to the mathematical modeling of the material based on its physical behavior through the use of differential equations. The resolution of these equations has traditionally been done via analytical or discretization methods, although more recently the validity of computational methods, such as deep neural networks, has also been demonstrated [1]. Another notable method employed in experimental optimization procedures of such strength performance is the Response Surface Method (RSM). RSM uses mathematical models and subsequent statistical analyses in experimental design, linking each strength response with a set of variables to assess the impacts and interactions of these parameters in the optimization process [2]. The advantages of using these tools extend far beyond achieving optimal results more rapidly [3]. Their application leads to a reduction in the consumption of raw materials, energy, and CO_2 emissions [4], thus fostering sustainability when they are employed [5].

The construction sector is widely acknowledged as a leading contributor to environmental degradation due to its extensive consumption of concrete and cement [6]. First, cement ranks as the second most consumed material globally, following water [7] and its calcination processes represent one of the largest sources of CO_2 emissions [8]. Furthermore, the considerable energy demand of the cement industry, which ranks as the third-largest energy consumer [6], exacerbates global warming and significantly impacts climate change. Another critical environmental concern associated with concrete production is the extraction and utilization of raw materials, especially Natural Aggregates (NA). The extraction of these resources has significant adverse environmental impacts, including habitat destruction, disruption of

Acronym glossary: RSM, Response Surface Method; RCA, Recycled Concrete Aggregates; NA, Natural Aggregates; RCWTB, Raw-Crushed Wind-Turbine Blade; CCD, Central Composite Design; ANOVA, ANalysis Of VAriance; ITZ, Interfacial Transition Zone.

* Corresponding author.
E-mail address: vrevilla@ubu.es (V. Revilla-Cuesta).

https://doi.org/10.1016/j.compstruct.2025.118895
Received 3 September 2024; Received in revised form 15 November 2024; Accepted 23 January 2025
Available online 25 January 2025

ecosystems, and depletion of natural resources essential for ecological balance [9].

These activities contribute further to the industry's overall environmental footprint and emphasize the urgent need for sustainable practices and innovation within the construction sector. To address this challenge, various strategies have been implemented. These practices include developing low-carbon alternative cements, such as Portland cement blended with supplementary cementitious materials like blast furnace slag or fly ash [10], and fiber addition [7]. Furthermore, significant progress has been made in researching alternative materials to replace NA, with Recycled Concrete Aggregates (RCA) emerging as a substitute [11]. Looking ahead, promoting the use of optimization tools like RSM, is critical to advocate for efficient material utilization in concrete mixtures. This approach involves optimizing sustainable material content to maximize mechanical properties while minimizing resource consumption and waste generation, aligning with sustainability and environmental goals [12].

RSM has been used in concrete mixes produced with RCA, evaluating its interaction with other factors, such as cement content [13] or combinations of recycled masonry aggregates with RCA [14]. Despite the inclusion of RCA in these models, it is not typically considered a factor to be optimized, and research studies focusing on RCA as a primary optimization factor remain limited [15]. In terms of optimizing fiber content, various studies have explored the incorporation of different fiber types in concrete mixtures, including basalt fiber [16], hybrid steel micro-fibers [17], forta-ferro fiber [18] and sisal fibers [19]. Therefore, there is currently a notable gap in research concerning the optimal combination of RCA and fibers in concrete mixtures, highlighting a critical area that requires further investigation.

The wind energy industry is currently facing a critical challenge in developing a sustainable waste management solution for decommissioned wind farms [20]. With the designated lifespan of wind turbines set at approximately 25 years and the imperative to repower specific wind farms, a substantial volume of waste is being produced, primarily consisting of turbine blades and foundation materials [21]. On the one hand, turbine blades exhibit a complex composition, comprising materials such as Glass Fiber-Reinforced Polymer (GFRP), balsa wood and polymeric particles [22]. To address this, various treatments, including mechanical and thermal processes, have been explored. Among these, non-selective cutting and milling has emerged as the most economically viable, energy-efficient, and environmentally responsible solution [23,24]. Prior investigations conducted by the authors of this study evaluated the efficacy of the shredding process and characterized the properties of the resulting material for use in concrete, referred to as Raw-Crushed Wind-Turbine Blade (RCWTB) [24]. This waste material is mainly composed of fibers from the crushing of the GFRP (66.8 % wt.) [25].

On the other hand, during the decommissioning process of wind turbines, a significant volume of waste originating from the foundations is also produced [26]. One promising approach to utilize this waste is advocated by the construction industry in the form of RCA. RCA, derived from screening, crushing, and sieving concrete waste, has been successfully integrated into concrete mixes [27], effectively reducing energy consumption and CO_2 emissions. However, its use leads to significantly different mechanical properties of concrete in comparison to NA [28]. Furthermore, due to the porous nature of adhered mortar, addition of RCA also has a major impact on workability [29], as adhered mortar absorbs water, resulting in the reduction of available water for the mixing [30]. Nevertheless, with up to 25 % of RCA replacement and the use of a superplasticizer, it is possible to achieve an optimum slump of the mixture [28]. Therefore, the material extracted from wind turbine foundations holds promise as an alternative for replacing NA, which constitute 75 % of the total volume of concrete [31].

Given that the wind sector is expected to generate the aforementioned materials in large quantities, the incorporation of these residues into concrete mixes is being studied as a recycling solution. The primary aim of this investigation is to use RSM optimization models to determine the optimal contents of RCA and RCWTB in these mixes. This approach not only enables the simultaneous utilization of both waste materials from the decommissioning of wind farms, but also transforms concrete into a more sustainable material while ensuring its mechanical performance. As part of this study, the properties of each concrete mix are analyzed in both the fresh and hardened state at 28 days of age, as detailed in sections 3.1, 3.2, and 3.3. Following the compilation and analysis of these results, optimization models are developed using RSM to evaluate two key mechanical properties of concrete: compressive strength and flexural strength, as explained in Section 4.

The novelty of the research presented in this article therefore lies in several points. First, the study of the behavior of concrete made with RCWTB is very limited, and it is necessary to study this aspect in more depth before establishing this method as a valid alternative for the recycling of wind-turbine blades. Second, the scientific literature does not currently include any study that addresses the 28-day strength behavior of concrete made simultaneously with RCA and RCWTB, which is key for the joint management and revaluation of both wastes from the decommissioning of wind farms as raw material in concrete. Finally, this is the first study dealing with the optimization of joint contents of RCA and RCWTB in concrete so that the resulting concrete's strength is valid for a wide range of applications in the construction and civil engineering sectors.

2. Materials and experimental methods

2.1. Materials

Regarding the materials used in the production of these mixtures, CEM II/A-L 42.5 R was employed in compliance with EN 197-1 [32] standard. This selection was based on its low limestone content, ranging from 6 % to 20 % by weight, aimed at minimizing its environmental impact [33]. Furthermore, in addition to regular tap water, superplasticizers were incorporated to enhance workability, while simultaneously maintaining low water/cement (w/c) ratios.

In relation to the aggregates used, various fractions of different nature were employed: limestone-based aggregates including fine sand 0/2 mm, and siliceous aggregates consisting of fractions 0/4 mm, 4/12 mm, and 12/22 mm. The physical properties of each fraction are defined in Table 1, and their size distributions are shown in Fig. 1 according to standard requirements.

The incorporation of recycled materials into the concrete mixes involved, on the one hand, the use of coarse RCA with a size of 4/22 mm, as depicted in Fig. 2a. This specific fraction was derived from the crushing and subsequent sieving of concrete elements sourced from a waste treatment company located in Burgos, Spain, where the investigation was conducted. The parent concrete elements had a minimum compressive strength of 45 MPa. Existing literature on the application of RCA has demonstrated its satisfactory utilization for structural elements [11] without compromising its mechanical behavior through a proper mix design. Comparative analysis with the same NA fraction revealed that this material exhibited lower density values, while demonstrating

Table 1
Physical properties of each fraction of the aggregates used (EN 1097-6 [34]).

Aggregate size	*Saturated-surface-dry density (kg/m^3)*	*24-hour water absorption (% wt.)*
Limestone 0/2 mm	2.66	0.10
Siliceous 0/4 mm	2.62	0.13
Siliceous 4/12 mm	2.63	0.33
Siliceous 12/22 mm	2.60	0.55
RCA 4/22 mm	2.44	6.12

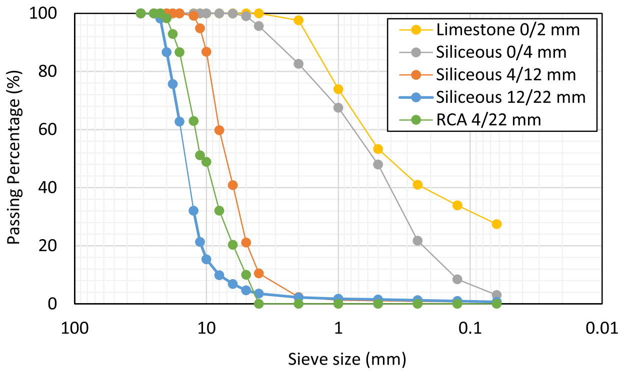

Fig. 1. Particle gradation of aggregates (EN 933-1 [32]).

significantly higher water absorption levels, reaching 6.12 % wt. (Table 1), as widely documented in the scientific bibliography [35].

The other recycled material added to the concrete mixes was RCWTB. Careful characterization was required to determine the specific role of each of its constituents on concrete mixes due to the diversity inherent in the composition of the RCWTB. Following the sectioning of central areas of wind turbine blades, rectangular panels measuring 20 cm × 30 cm were obtained and subjected for further crushing using a knife mill [24]. The resulting material was sieved to obtain RCWTB, which consists of GFRP-composite fibers with polymeric and balsa wood particles. Within the concrete mixtures, GFRP-composite fibers are expected to provide a stitching effect, while the polymeric and balsa wood particles would function as aggregates [25,36]. Visual representation provided in Fig. 2b illustrates the heterogeneity associated with RCWTB, providing insight into the variation among its constituent elements. In terms of its physical properties, the material exhibited a real density of 1.63 kg/dm^3 as determined by EN 1097-6 [32] and a fiber content of 66.8 % by weight. Both the production process of RCWTB and its resulting properties have been extensively investigated in previous research by the authors [24].

2.2. Mix design

Thirteen different mixture designs were conducted with varying contents of RCWTB ranging from 0 % to 10 % of the aggregate volume, and RCA ranging from 0 % to 100 % of the volume of coarse aggregate. The selection of these ranges was informed by findings from the existing literature on concrete incorporating these materials. Previous studies conducted by the authors of this paper indicated that RCWTB, when used within the range of 0 % to 6 % of the concrete volume, can positively influence properties like workability and durability without compromising strength [37,38]. Similarly, RCA, utilized between 0 % and 100 % for NA substitution, has shown varied effects on concrete strength and durability depending on its quality and processing, as discussed in the comprehensive review of Makul *et al.* [39].

The selection of combinations of both residues was based on the Central Composite Design (CCD) model with two variables (k = 2) to obtain corresponding optimized response surfaces in subsequent phases of the research. In the present study, the impact of each factor was evaluated by ensuring that the variance of the response predicted by the model depended solely on the distance from the center of the modelled region. Therefore, α values of ±0.5 and ±1 were considered. Fig. 3 illustrates the combinations obtained for each concrete mixture. All mixtures were labelled as *WxRCAx*, where *Wx* represented the RCWTB percentage content, and *RCAx* represented the percentage of coarse RCA incorporated. Within this model, four replicates of the central point corresponding to the mixture *W5RCA50* were performed to evaluate the variability of the strength performance of concrete, resulting in a total of 16 experimental mixtures.

Initially, a mixture designed as a reference (*W0RCA0*) was executed, characterized by the absence of both types of recycled materials. The composition of the reference mix is defined in Table 2. It was formulated using the materials detailed in Section 2.1, aiming to achieve slump and strength parameters suitable for its application in structural concrete. In accordance with the stipulations of EUROCODE 2 [34], the cement content within the mixture was fixed at 320 kg/m^3, accompanied by a w/c ratio of 0.40. Additionally, the superplasticizers content was set at 1 % relative to the total mass of cement. The proportions of aggregate fractions were defined for adjustment based on the Fuller's curve, as depicted in Fig. 4. Following the definition of the reference mixture design, coarse NA was replaced with the amount of coarse RCA specified for each mixture by volume correction. The incorporation of RCWTB was considered as an addition to the cement content, where the volume of cement added remained constant in all manufactured mixtures.

The increased water-absorption capacity of RCA generally leads to a reduction in workability [40], with the main determining factor being the moisture state in which it is introduced into the mixing process [35].

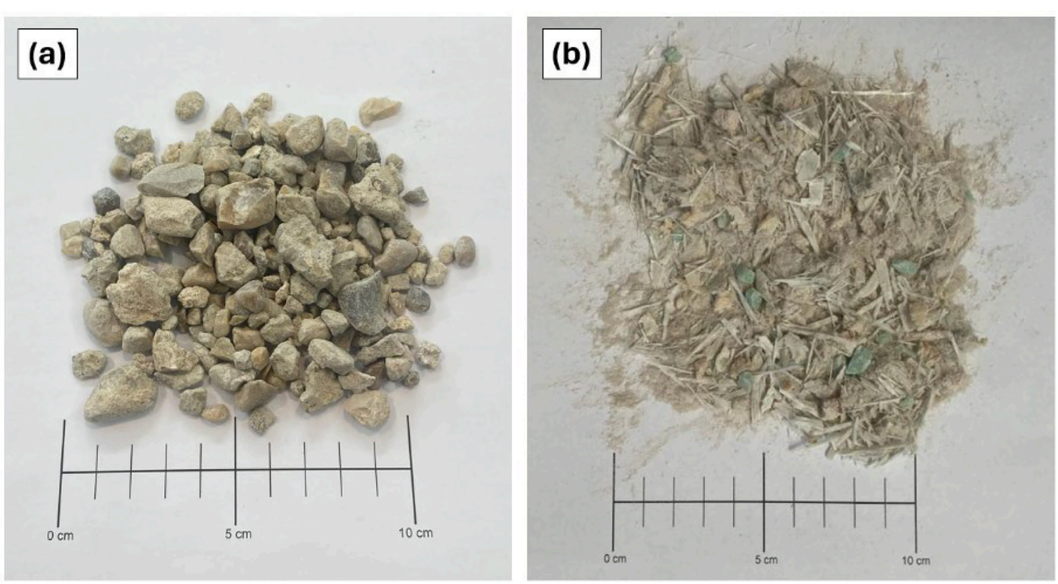

Fig. 2. Recycled materials: (a) RCA 4/22 mm; (b) Raw-Crushed Wind-Turbine Blade.

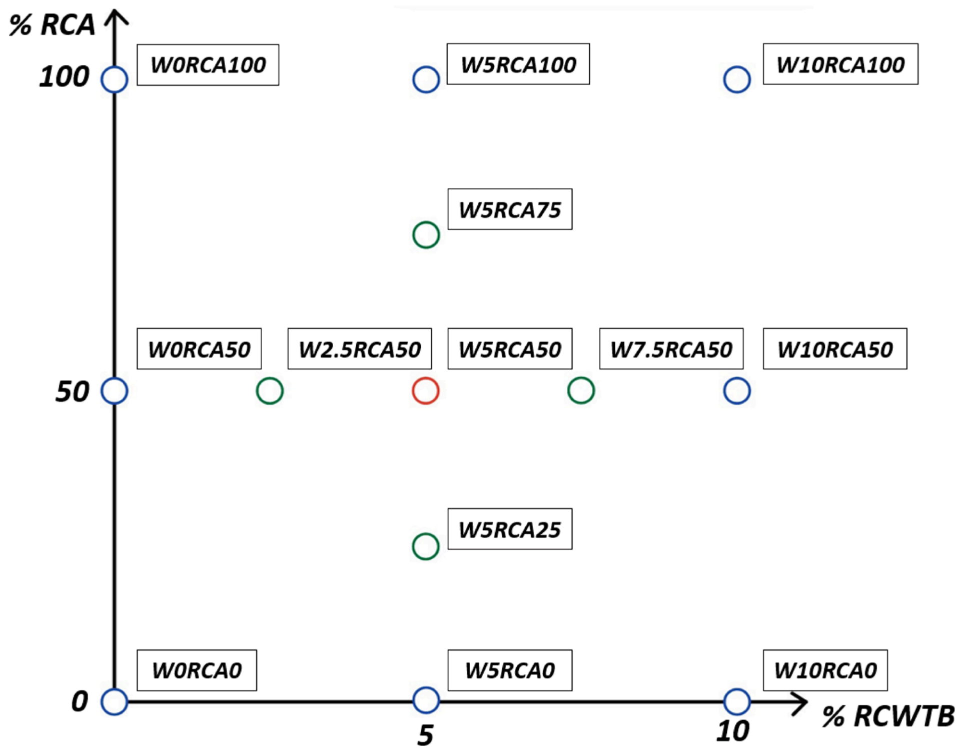

Fig. 3. Combination of RCA and RCWTB for the production of concrete for a CCD with k = 2 and α values of 0.5 and 1.

Table 2
Composition of the reference mixture (kg/m^3).

MIXTURE	*Cement*	*Water*	*Superplasticizers*	*Gravel 12/22*	*Gravel 4/12*	*Sand 0/4*	*Sand 0/2*
Reference	320	12	3.20	780	555	385	280

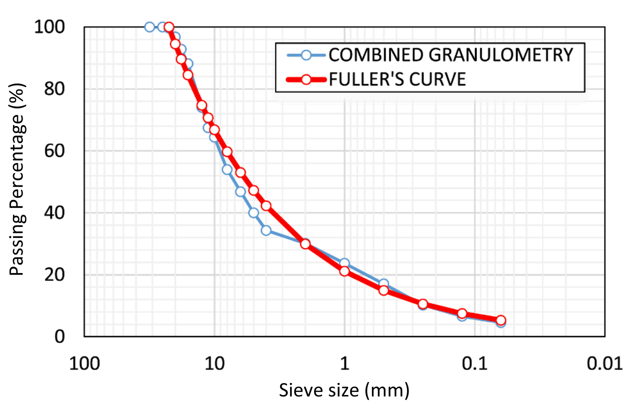

Fig. 4. Combined granulometry of the concrete mixes and adjustment of Fuller's Curve.

Furthermore, the fibers present in the RCWTB could hinder the flow of the other concrete components, which also reduced workability [41]. The mixtures in this investigation were meticulously formulated to consistently achieve a S3 slump classification (EN 206 [32]). This required empirical adjustments of water and superplasticizers for each mixture, thus counteracting the loss of workability due to the incorporation of both waste materials [42]. Superplasticizers served the purpose of reducing the water requirement in the mixing process, while concurrently upholding the w/c ratio of the mixtures in close proximity to the reference mixture value of 0.40. Adjustments for water and superplasticizers were implemented as follows:

- For mixtures containing 0 % and 5 % RCWTB, the total water content was increased on average by 14 L/m^3 for each 50 % increment in coarse RCA. No adjustment was required for the admixtures.
- For mixtures with higher RCWTB contents, specifically those with 10 % RCWTB, the same additional amount of water was added for each 50 % increment in coarse RCA. Furthermore, the superplasticizers content was also adjusted, increasing to 4.02 kg for the mixture *W10RCA0* and to 4.26 kg for the mixtures *W10RCA50* and *W10RCA100*.

2.3. Concrete preparation

The mixing process was carried out in three stages. Initially, all NA fractions were combined in a vertical axis mixer with the coarse RCA, along with 30 % of the water, reserving 0.5L for a subsequent phase. The incorporation of the RCA at this stage ensures adequate moisture state of the RCA, which, when integrated with the water, eliminates the need to increase the total water content of the mix to compensate for the higher water absorption capacity of the adhered mortar [43,44]. After three minutes of mixing, RCWTB was added with the cement, along with the remaining 70 % of the water. Thus, adequate cement hydration and proper RCWTB distribution within the concrete mass was reached [45]. Following another three minutes of mixing, the superplasticizers dissolved in the previously reserved 0.5L of water were introduced. The mixture was considered ready for fresh property testing and casting after three minutes of further mixing in the final stage. Fig. 5 schematically illustrates the manufacturing process used for the mixture production.

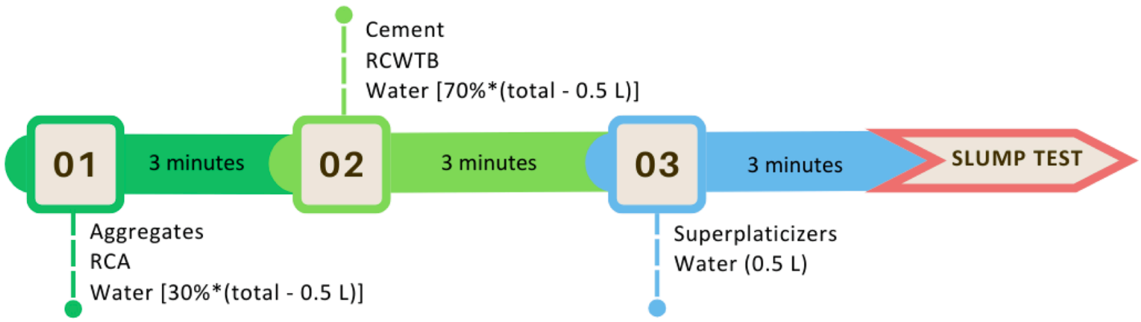

Fig. 5. Three stage mixing process for concrete mixtures preparation.

2.4. Test procedures

In pursuit of the main objectives of this research, a series of tests were conducted on each mix to fully evaluate its properties. Immediately after the mixing process was completed, three tests were performed to evaluate the fresh-state properties, in accordance with the outlined by the EN standards [32]: slump test (EN 12350-2), fresh density test (EN 12350-6), and air content test (EN 12350-7). Moreover, the evaluation of hardened-state properties involved the casting various specimens. For the assessment of compressive strength in accordance with EN 12390-3, cylindrical specimens sized at 100 × 200 mm were employed. Additionally, to evaluate flexural strength as per EN 12390-5, prismatic specimens measuring 75 × 75 × 275 mm were used. In each experiment, three specimens were fabricated for every type of mixture and stored inside a moist room (EN 12390-2) until they reached the established age for testing (28 days).

3. Results and discussion: Experimental properties

3.1. Fresh properties

The workability of all concrete mixes was assessed through the slump test, as this property is usually negatively influenced by the incorporation of RCA and RCWTB [46,47]. The reference mixture exhibited a slump value of 14.7 cm, classified as S3 according to EN 206 [32]. The remaining mixtures showed slump values ranging from 10 to 15 cm, as shown in Fig. 6a, with all successfully achieving an S3 classification. Thus, the range of desired slump values implies that workability did not influence the outcome of the mechanical properties of the mixtures, attributing this behavior to other factors [25].

A decrease in workability was evidenced by the increase in RCA content, attributed to the higher water absorption values as well as rougher texture of the coarse RCA in contrast to NA, which led to an increase in the water demand by the mixture [43]. Fig. 6a illustrates that those mixtures containing 100 % RCA exhibited the lowest slump values, regardless of the amount of RCWTB, with W*0RCA100* mixture,

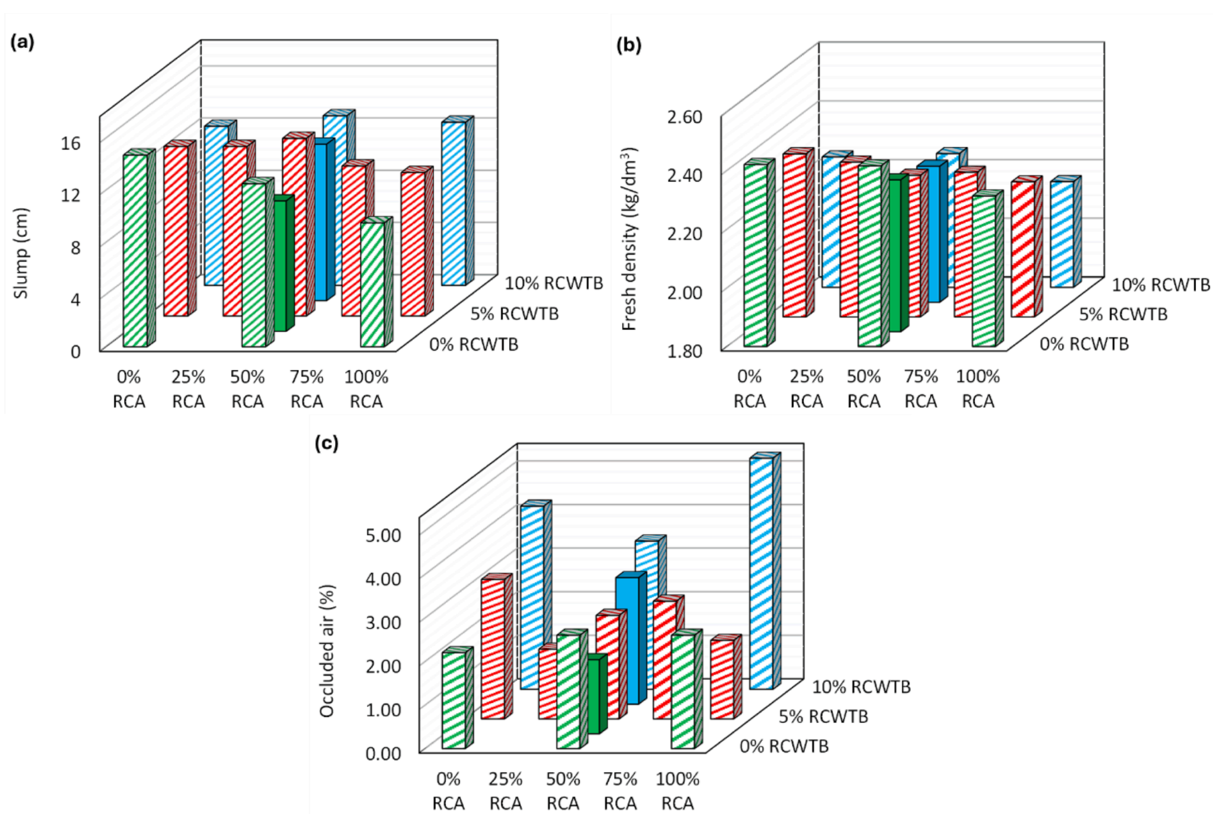

Fig. 6. Fresh properties: (a) slump; (b) fresh density; (c) air content.

for example, having a slump of only 9.5 cm.

Regarding the incorporation of RCWTB, there was no clear trend indicating a decrease in slump with increasing RCWTB content, as might have been expected. While all mixtures exhibited lower slumps compared to the reference mixture, an increase in slump was observed for some mixtures containing 5 % and 10 % RCWTB compared to mixes with lower RCWTB amounts. The *W5RCA50* mix achieved a slump value of 13.6 cm, closely matching the reference mixture, and the *W10RCA100* mixture exhibited a higher workability (12.5 cm) than that of mixtures with lower fiber content. The effect of the GFRP-composite fibers of the RCWTB opposing the flow of the other concrete components [48] was likely compensated by the increased content of water and superplasticizers in the concrete [49], which effectively coated the specific surface area of the RCWTB components.

Fresh density values are presented in Fig. 6b. A decrease was observed with the increasing addition of both residues, from 2.42 kg/dm^3 for the reference mix (*W0RCA0*) to 2.16 kg/dm^3 for the mix containing the highest proportions of RCA and RCWTB, *W10RCA100*. The 4.55 % reduction for *W0RCA100* may be attributed to the lower density of RCA compared to NA [35]. Similarly, the components of RCWTB exhibit very low densities [36], further decreasing the fresh density of the resultant concrete.

Finally, the results for the air content are presented in Fig. 6c. The incorporation of RCWTB, along with the substitution of coarse aggregate fractions with RCA, negatively impacted the air content, yielding an extreme value of 5.30 % in *W10RCA100*, which is double that of the reference mixture. This increment can be mainly attributed to the higher porosity of the RCA [50]. Furthermore, the presence of fibers in the RCWTB enhances air retention within the cementitious matrix [25], meanwhile the balsa wood particles in the RCWTB lead to the formation of more porous Interfacial Transition Zones (ITZs) [51]. The combined effects of both wastes when added simultaneously to concrete resulted in an air content of 3.40 % observed in *W10RCA50*.

3.2. Compressive strength

The compressive strength was evaluated at 28 days to study the effect of adding both residues on this property. Its average values are represented in Fig. 7a, while Table 3 lists them along with the standard deviations. All the individual experimental results can be found in the supplementary material. Furthermore, it can be noted that all the mixes exhibited similar levels of standard deviation (Table 3), the results being therefore reliable and suitable for the development of statistical models.

As an initial requirement for the mixtures to be used as structural concrete, a minimum compressive strength value of 25 MPa at this age was targeted. This threshold was indeed achieved in all the mixtures manufactured, for all combinations of residues. In general terms, the observed trend was consistent with other evaluated properties, showing

Table 3
Compressive strength values of the concrete mixes [MPa]: average values and standard deviations.

		RCWTB (%)				
		0 %	***2.5 %***	***5 %***	***7.5 %***	***10 %***
RCA (%)	***0 %***	47.22 ± 3.36		40.91 ± 3.99		39.33 ± 2.83
	25 %			44.98 ± 1.77		
	50 %	48.18 ± 1.61	39.47 ± 0.98	41.87 ± 1.68	38.94 ± 1.85	42.48 ± 0.78
	75 %			36.68 ± 1.82		
	100 %	43.66 ± 1.29		36.66 ± 3.60		26.84 ± 2.05

a decrease in compressive strength as the contents of RCA and RCWTB increased. However, some specific observations are necessary to draw further relevant conclusions:

- For mixtures with 0 % RCWTB, 50 % RCA led to an increase in compressive strength of around 1 MPa, although a decrease of approximately 3.60 MPa was found when adding 100 % RCA. On the other hand, the trend was different in mixtures without RCA but with increased RCWTB contents. In this case, the decrease in compressive strength was more pronounced, with a reduction of 3.94 MPa for each additional 5 % of RCWTB.
- The *W0RCA50* mixture increased its compressive strength by nearly 1 MPa compared to the reference mixture; a similar improvement was observed for *W5RCA25* mixture, which exhibited a 9 % increase in strength compared to the mixture with 5 % RCWTB and without RCA substitution. Therefore, low (25–50 %) RCA contents led to increases in compressive strength in some cases.
- The lowest compressive strength value was observed in the *W10RCA100* mixture, which contained the highest combination of both residues. The loss of strength was 57 % compared to the reference mixture.

The behavior of the mixtures in terms of compressive strength can be attributed to the following observations:

- The slight reduction and in some case increase in compressive strength observed in mixtures exclusively incorporating RCA could be thanks to the high quality of the parent concrete, which originally had a compressive strength of 45 MPa. This superior feature of the RCA likely contributed to the resulting mixtures' higher strength values [52,53], with some even surpassing the reference mixture, as in the case of *W0RCA50*. The quality of the parent concrete is

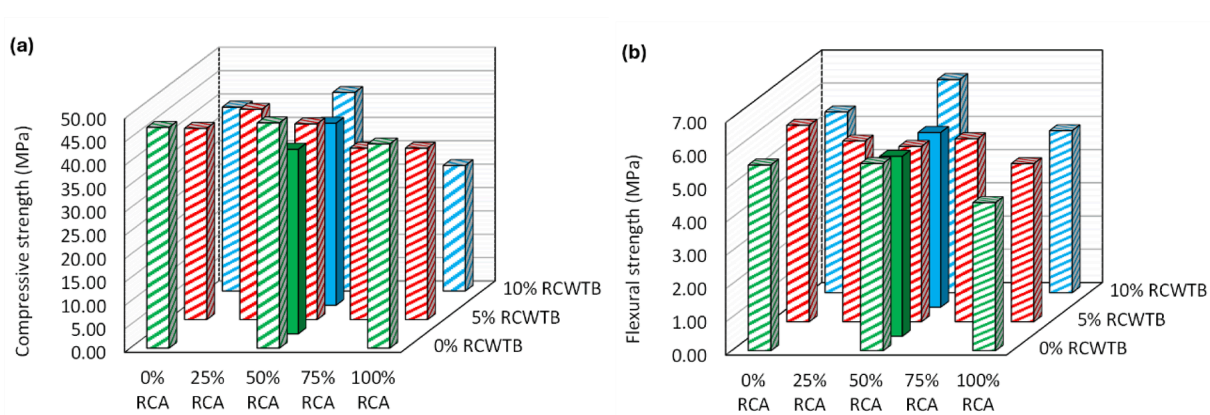

Fig. 7. Mechanical-behavior properties: (a) compressive strength; (b) flexural strength.

considered to be a determinant factor for compressive strength outcomes, as supported by other research [54].

- On the one hand, the incorporation of both RCA and RCWTB required an adjustment in the w/c ratio of the mixtures, which resulted in increased total water content. Consequently, effective w/c ratios reached a maximum value of 0.58 for the *W10RCA100* mixture, leading to a reduction in compressive strength values [55].
- On the other hand, the more pronounced reduction in strength values was attributed to the high porosity of the RCA [56]. This property was exacerbated by the presence of old ITZ and adhered cement mortar from the parent concrete from which the RCA is extracted [57,58].
- High content of RCWTB was responsible for the marked losses observed in mixes containing this residue, as the proportion of weak particles, such as the polymeric and balsa wood ones, was higher. This fact, along with the reduced adhesion of these particles to the cementitious matrix [59], lead to significant reductions in compressive strength values.

3.3. Flexural strength

The flexural behavior of the mixes was evaluated through the flexural strength test (EN 12390-5) [32]. The average results of this test are shown in Fig. 7b. Moreover, Table 4 lists the average values with their standard deviations, and all the individual experimental results are shown in the supplementary material. Similar values of standard deviation were obtained in all the mixtures, the validity of these results for statistical-model development being verified.

The main observations regarding this behavior are as follows:

- In general, as the percentage of RCA substitution increased, a decrease in strength values was observed due to the weak ITZs it generated [60,61]. In fact, the *W0RCA100* mix experienced a strength loss of 20.21 % compared to the *W0RCA0* mix. Contrariwise, the addition of the fibers present in the RCWTB to the concrete, improved flexural strength, which can be attributed to their stitching effect within the cementitious matrix [62].
- The most notable increase relative to the reference mix was achieved by *W10RCA50* mixture, which exhibited a 14.67 % increase in strength. This mix showed the optimum performance of the GFRP-composite fibers with that amount of coarse RCA, as observed in studies evaluating this waste material at an early age of the mixture [37], highlighting the prospective capabilities of simultaneously using both recycled materials in concrete. Fig. 8. illustrates the performance of a specimen used for the flexural test for that concrete mixture, showing the pre-test phase, the test phase and the post-failure phase; it can be observed that a crack appeared in the central part of the specimen, a failure of the specimen in a proper way was obtained, and the specimen exhibited load-bearing capacity.

Table 4
Flexural strength values of the concrete mixes [MPa]: average values and standard deviations.

		RCWTB (%)				
		0 %	***2.5 %***	***5 %***	***7.5 %***	***10 %***
RCA (%)	***0 %***	5.59 ± 0.52		5.91 ± 0.56		5.44 ± 0.35
	25 %			5.44 ± 0.45		
	50 %	5.64 ± 0.56	5.42 ± 0.50	5.28 ± 0.28	5.26 ± 0.07	6.41 ± 0.34
	75 %			5.51 ± 0.21		
	100 %	4.46 ± 0.58		4.76 ± 0.13		4.88 ± 0.28

Despite the general trends indicated, both wastes exhibited an interaction in terms of flexural strength. For instance, the mixtures with a RCWTB content of 5 % either improved or maintained values of flexural strength close to the reference mix for low RCA substitutions, but a notable deterioration with complete replacement of NA by RCA was found. The addition of RCA led to the creation of weak ITZs with increased porosity [63], which may negatively impact flexural strength [64]. Nevertheless, for low w/c ratios, this effect was mitigated due to the stitching effect of the GFRP-composite fibers, as seen in mixtures with less than 50 % RCA substitution. In mixtures requiring increased water and admixtures adjustment, the losses were significantly higher, the fibers not being so effective. Therefore, the effects caused by adjustments in the w/c ratio [63,65] or the increased porosity because of RCA addition [66] were offset by the stitching effect of the fibers [38,67] up to RCA amounts of 50 %, which also prevented crack propagation within the matrix [68]. The presence of RCA with high parent concrete strength could also contribute to the flexural-strength improvements observed [69].

4. Optimization by response surface method

4.1. Initial considerations

Design Expert software version 13.0.5 was employed for the optimization through RSM in this research. Initially, the independent variables (factors) and dependent variables (responses) pertinent to the study were defined, followed by the design of the models.

The following key points were considered regarding the factors and the responses in RSM application:

- The percentage replacement of NA with coarse RCA and the percentage addition of RCWTB were used as factor variables. The upper and lower ranges for these input parameters were set at 0–100 % for RCA replacement and 0–10 % for RCWTB addition.
- CCD was selected for its widespread application in RSM to establish the relationship between factors and responses in concrete mixtures [12]. The CCD resulted in a total of 16 experimental runs (mixtures), with each factor ($k = 2$) varying at 5 levels. These levels were defined by the following α values: $+0.5$ and -0.5 (axial points), $+1$ and -1 (factorial points), and 0 (center point) as summarized in Table 5. To assess the experimental error, four replicate center points were included. These aspects were also outlined in section 2.2 for a proper understanding of the mixes design.
- Compressive strength and flexural strength were set as response variables. Their values, which were used to RSM adjustment, can be found in Fig. 7, Table 3 and Table 4. However, in the mixes containing wastes with higher variability in flexural strength and located at the limits of the CCD space, the extreme experimental individual values were considered following the trend of the rest of the mixes as an additional safety factor.

For the development of the mathematical models, the following Eqs. (1) and (2) were used:

$$Y = \beta_0 + \sum_{i=1}^{k} \beta_i X_i + \varepsilon_0, \tag{1}$$

$$Y = \beta_0 + \sum_{i=1}^{k} \beta_i X_i + \sum_{i=1}^{k} \beta_{ii} X_i^2 + \sum_{i=1}^{k} \sum_{j>1}^{k} \beta_{ij} X_i X_i + \varepsilon_0, \tag{2}$$

where Y represents the response; β represents the regression coefficients; X_i represents the factor or independent variables; k represents the number of optimized variables; and ε_0 refers to the measured error. In cases where the response could be modelled by a function represented as

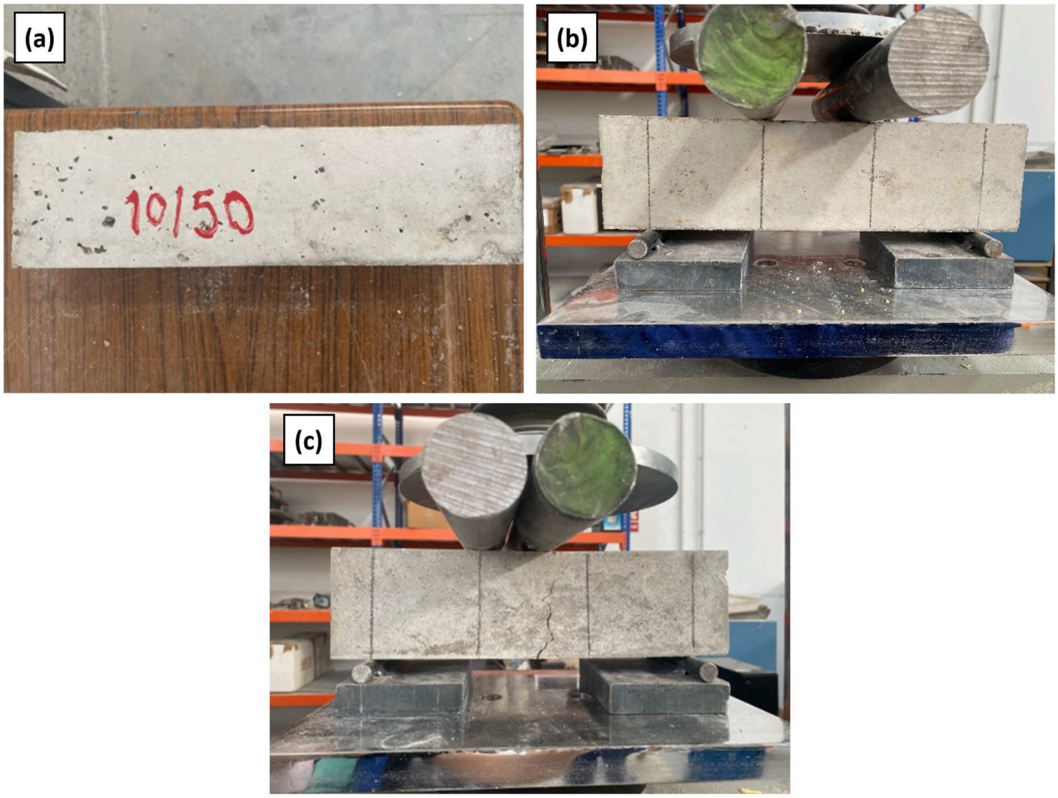

Fig. 8. (a) Prismatic specimen before conducting the flexural strength test; (b) flexural strength test; (c) result of the flexural fracture after the test, and load-bearing capacity of the *W10RCA50* mixture.

Table 5
Independent variables and coded values.

Coded values	*−1*	*−0.5*	*0*	*0.5*	*1*
% RCA	0	25	50	75	100
% RCWTB	0	2.5	5	7.5	10

a linear combination of the factors, that is, a first-order model, the function took the form of Eq. (1). For models exhibiting curvature, the corresponding equation for a second-order model, Eq. (2), was defined. Both a first-order (linear) and a second-order (quadratic) model for the optimization of RCWTB and RCA materials were developed for each response (compressive strength and flexural strength) and α value (±0.5 and ±1). These models were subsequently subjected to an ANalysis Of VAriance (ANOVA) and compared to assess their efficacy in the optimization process, thus selecting a single model for each strength property and each α value (4 selected models). Finally, the models for each property (one for an α value of ±0.5 and another for an α value of ±1) were compared, selecting only one for compressive strength and one for flexural strength, which were used for the final optimization. The detailed methodology and results are presented in the following sections.

4.2. Statistical analysis results of the RSM

Regression analyses were conducted to establish the relationships between factors and responses, considering the two fixed α values, α = ± 1 and α = ± 0.5; both linear and quadratic regression models were considered for each α value. An ANOVA was conducted in each case for statistical validation. Hypothesis tests on the significance of the model terms were developed to evaluate the sensitivity of each one of them in relation to the variability of the experimental data. In this way, statistically non-significant terms were detected, as only model variables with a *p-value* under 0.05 (confidence level of 95 %) were considered significant terms. In addition, the overall significance of the model was also evaluated, and a lack-of-fit hypothesis test was performed to ensure adequate model adjustment regardless of the data variability. Finally, the R^2 coefficient of each model was also assessed.

4.2.1. Response: Compressive strength

Table 6 presents the ANOVA corresponding to compressive strength (α = ± 1). It can be observed that the linear model was significant (*p-value* = 0.0178), moreover showing that variable A (% RCWTB), with a *p-value* of 0.0149, had a significant effect on compressive strength, while variable B (% RCA), with a *p-value* of 0.0759, did not. Analysis of R^2 = 0.5917 and Adj-R^2 = 0.5010 suggested that the model explained approximately 59.17 % of the variability in strength, with the lack-of-fit analysis indicating adequate model fit to the observed data (*p-value* = 0.4981).

Regarding the quadratic model, it was significant overall (*p-value* = 0.0341). Evaluating each variable independently, parameters A and B, as well as the interaction B^2 showed a significant effect (*p-values* of 0.0110, 0.0418 and 0.0488), while the interactions AB and A^2 and did not. It was concluded that the quadratic model fitted better than the linear model, with an R^2 of 0.8133 and Adj-R^2 of 0.6577, explaining approximately 81.33 % of the variability in compressive strength. Lack-of-fit analysis was not significant (*p-value* = 0.7109), indicating adequate fit of the quadratic model to the observed data, thereby selecting this model for the optimization process when α = ± 1.

In the comparative analysis of models for compressive strength when α = ± 0.5 (Table 7), the linear model demonstrated overall significance (*p-value* = 0.0045). Both A and B were significant with *p-values* of 0.0062 and 0.0183, respectively, suggesting significant contributions to the observed variability. The model had an R^2 of 0.6992 and Adj-R^2 of 0.6323, explaining approximately 69.92 % of the variability in compressive strength, and showing good fit based on lack-of-fit analysis

Table 6
ANOVA on the effect of RCWTB and RCA for compressive strength (α = ± 1).

Dependent variable	Source	*df*	Sum of squares	F-value	p-value	Remark	R^2	Adj-R^2	Predicted R^2	Adequate Precision
Compressive strength (α = ± 1) / Linear response surface model	Model	2	222.81	6.52	0.0178	**Sign.**	0.5917	0.5010	0.2257	8.1794
	A: % RCWTB	1	154.13	9.02	0.0149	**Sign.**				
	B: % RCA	1	68.68	4.02	0.0759	**Not-Sign.**				
	Residual	9	153.75							
	Lack of fit	6	106.72	1.13	0.4981	**Not-Sign.**				
	Pure error	3	47.03							
	Cor Total	11	376.56							
Compressive strength (α = ± 1) / Quadratic response surface model	Model	5	306.26	5.23	0.0341	**Sign.**	0.8133	0.6577	0.1969	8.5243
	A: % RCWTB	1	154.13	13.15	0.0110	**Sign.**				
	B: % RCA	1	68.68	5.86	0.0418	**Sign.**				
	AB	1	19.94	1.70	0.2399	**Not-Sign.**				
	A^2	1	7.39	0.6309	0.4573	**Not-Sign.**				
	B^2	1	63.51	5.42	0.0488	**Sign.**				
	Residual	6	70.30							
	Lack of fit	3	23.27	0.4949	0.7109	**Not-Sign.**				
	Pure error	3	47.03							
	Cor Total	11	376.56							

Table 7
ANOVA on the effect of RCWTB and RCA for compressive strength (α = ± 0.5).

Dependent variable	Source	*df*	Sum of squares	F-value	p-value	Remark	R^2	Adj-R^2	Predicted R^2	Adequate Precision
Compressive strength (α = ± 0.5) / Linear response surface model	Model	2	229.29	10.46	0.0045	**Sign.**	0.6992	0.6323	0.3551	12.1281
	A: % RCWTB	1	138.61	12.64	0.0062	**Sign.**				
	B: % RCA	1	90.68	8.27	0.0183	**Sign.**				
	Residual	9	98.66							
	Lack of fit	6	59.35	0.7550	0.6491	**Not-Sign.**				
	Pure error	3	39.31							
	Cor Total	11	327.95							
Compressive strength (α = ± 0.5) / Quadratic response surface model	Model	5	261.05	4.68	0.0435	**Sign.**	0.7960	0.6260	−1.6880	8.5033
	A: % RCWTB	1	138.61	12.43	0.0124	**Sign.**				
	B: % RCA	1	90.68	8.13	0.0291	**Sign.**				
	AB	1	19.94	1.79	0.2296	**Not-Sign.**				
	A^2	1	4.37	0.3915	0.5546	**Not-Sign.**				
	B^2	1	1.25	0.1123	0.7490	**Not-Sign.**				
	Residual	6	66.90							
	Lack of fit	3	27.59	0.7020	0.6109	**Not-Sign.**				
	Pure error	3	39.31							
	Cor Total	11	327.95							

(*p-value* = 0.6491). Conversely, the quadratic model was also significant (*p-value* = 0.0435), with A and B significant with *p-values* of 0.0124 and 0.0291, respectively, unlike the interactions. An R^2 of 0.7960 and Adj-R^2 of 0.6260 indicated that the quadratic model explained approximately 79.60 % of the variability and showed adequate fit (*p-value* = 0.6109) according to lack-of-fit analysis. Although both models confirmed the importance of both % RCWTB and % RCA in compressive strength, the linear model was chosen in this case for its superior fit and simplicity.

4.2.2. Response: Flexural strength

For the analysis of flexural strength with α = ± 1 (Table 8), the linear response surface model was not significant overall (*p-value* = 0.7624), indicating that neither variable A nor B individually significantly affected flexural strength, with *p-values* of 0.6571 and 0.5695, respectively. The model's R^2 was 0.0585 and Adj-R^2 was −0.1507, suggesting lack of fit to the observed data (*p-value* = 0.0894), although this was not statistically significant. The quadratic response surface model, however, was significant overall (*p-value* = 0.0268). While A^2 (*p-value* = 0.0049) and B^2 (*p-value* = 0.0069) showed significant effects, neither A, B, nor their interaction AB significantly influenced flexural strength. Quadratic model exhibited an R^2 of 0.8289 and Adj-R^2 of 0.6862, indicating that it explained approximately 82.89 % of the variability in flexural strength.

Table 8
ANOVA on the effect of RCWTB and RCA for flexural strength (α = ± 1).

Dependent variable	Source	*df*	Sum of squares	F-value	p-value	Remark	R^2	Adj-R^2	Predicted R^2	Adequate Precision
Flexural strength (α = ± 1) / Linear response surface model	Model	2	0.1755	0.2796	0.7624	**Not-Sign.**	0.0585	−0.1507	−0.6593	1.7136
	A: % RCWTB	1	0.0662	0.2108	0.6571	**Not-Sign.**				
	B: % RCA	1	0.1094	0.3484	0.5695	**Not-Sign.**				
	Residual	9	2.82							
	Lack of fit	6	2.60	5.77	0.0894	**Not-Sign.**				
	Pure error	3	0.2253							
	Cor Total	11	3							
Flexural strength (α = ± 1) / Quadratic response surface model	Model	5	2.49	5.81	0.0268	**Sign.**	0.8289	0.6862	0.1093	8.4115
	A: % RCWTB	1	0.0662	0.7729	0.4131	**Not-Sign.**				
	B: % RCA	1	0.1094	1.28	0.3015	**Not-Sign.**				
	AB	1	0.0552	0.6453	0.4524	**Not-Sign.**				
	A^2	1	1.61	18.84	0.0049	**Sign.**				
	B^2	1	1.39	16.27	0.0069	**Sign.**				
	Residual	6	0.5135							
	Lack of fit	3	0.2882	1.28	0.4222	**Not-Sign.**				
	Pure error	3	0.2253							
	Cor Total	11	3							

Lack of fit analysis (*p-value* = 0.4222) suggested the quadratic model fitted adequately to the observed data. Therefore, despite the lack of significance in individual variables in the models, the quadratic model demonstrated superior predictive capability in relation to flexural strength and was therefore taken as the model for flexural strength optimization when α = ± 1.

For flexural strength with α = ± 0.5, the linear response surface model (Table 9) showed overall significance with a *p-value* of 0.0456. However, upon analyzing individual variables, only variable B (% RCA) was significant with a *p-value* of 0.0160. Variable A (% RCWTB), on the other hand, was not significant (*p-value* = 0.7418). The model's R^2 was 0.4965 and Adj-R^2 was 0.3847, suggesting moderate explanatory power; a lack of fit analysis (*p-value* = 0.5083) indicated that the model adequately fitted the observed data. In contrast, quadratic response surface model was not significant overall with a *p-value* of 0.1273. While variable B was significant with a *p-value* of 0.0211, variable A, and their interactions AB, A^2 and B^2 did not significantly influence flexural strength (all *p-values* > 0.3). Quadratic model exhibited an R^2 of 0.6941

Table 9
ANOVA on the effect of RCWTB and RCA for flexural strength (α = ± 0.5).

Dependent variable	Source	*df*	Sum of squares	F-value	p-value	Remark	R^2	Adj-R^2	Predicted R^2	Adequate Precision
Flexural strength (α = ± 0.5) / Linear response surface model	Model	2	0.6167	4.4400	0.0456	**Sign.**	0.4965	0.3847	−0.1735	6.2220
	A: % RCWTB	1	0.0080	0.1155	0.7418	**Not-Sign.**				
	B: % RCA	1	0.61	8.7600	0.0160	**Not-Sign.**				
	Residual	9	0.63							
	Lack of fit	6	0.4304	1.1000	0.5083	**Not-Sign.**				
	Pure error	3	0.1949							
	Cor Total	11	1.24							
Flexural strength (α = ± 0.5) / Quadratic response surface model	Model	5	0.8621	2.72	0.1273	**Not-Sign.**	0.6941	0.4392	−3.2081	5.7373
	A: % RCWTB	1	0.0080	0.1267	0.7341	**Not-Sign.**				
	B: % RCA	1	0.6087	9.61	0.0211	**Sign.**				
	AB	1	0.08	1.28	0.3006	**Not-Sign.**				
	A^2	1	0.04	0.5971	0.4690	**Not-Sign.**				
	B^2	1	0.0052	0.0821	0.7841	**Not-Sign.**				
	Residual	6	0.3799							
	Lack of fit	3	0.1850	0.9491	0.5166	**Not-Sign.**				
	Pure error	3	0.1949							
	Cor Total	11	1.24							

and Adj-R^2 of 0.4392, indicating it explained approximately 69.41 % of the variability. After this exhaustive analysis, the linear model was determined as the one that showed the greatest significance in the predictive capacity of the response.

4.2.3. Joint analysis of both responses

According to the conclusions derived from the ANOVA, the quadratic model was chosen for the optimization of compressive strength with $\alpha = \pm 1$, while the linear model was selected for $\alpha = \pm 0.5$. Numerically, these models predicted the value of compressive strength (*R1*, in MPa) using the following Eqs. (3) and (4), respectively:

$$R1 = +42.87 - 5.07 \times A - 3.38 \times B - 2.23 \times AB + 1.67 \times A^2 - 4.88 \times B^2 \tag{3}$$

$$R1 = +40.38 - 5.55 \times A - 4.49 \times B \tag{4}$$

For the case of flexural strength (*R2*, in MPa), following the same ANOVA criteria, the quadratic model was selected for $\alpha = \pm 1$, and the linear model was chosen for $\alpha = \pm 0.5$. The equations for each model are given by Eqs. (5) and (6):

$$R2 = +5.39 - 0.11 \times A - 0.14 \times B - 0.12 \times AB + 0.78 \times A^2 - 0.72 \times B^2 \tag{5}$$

$$R2 = +5.26 - 0.0422 \times A - 0.3678 \times B \tag{6}$$

Subsequently, if the estimation accuracy is analyzed, it is found that the models developed for $\alpha = \pm 1$ showed higher R^2 coefficients (0.81 for compressive strength and 0.83 for flexural strength, respectively, versus 0.70 and 0.50 of the models for $\alpha = \pm 0.5$). Furthermore, the *p-values* of the lack-of-fit tests were similar for the models corresponding to both α values. Thus, it was concluded that the use of $\alpha = \pm 1$ with quadratic models for fitting the response variables, Eqs. (3) and (5), was the optimal RSM procedure for obtaining accurate results in this case.

Contour lines and 3D graphs of the quadratic models for compressive strength and flexural strength when $\alpha = \pm 1$ are depicted in Fig. 9.

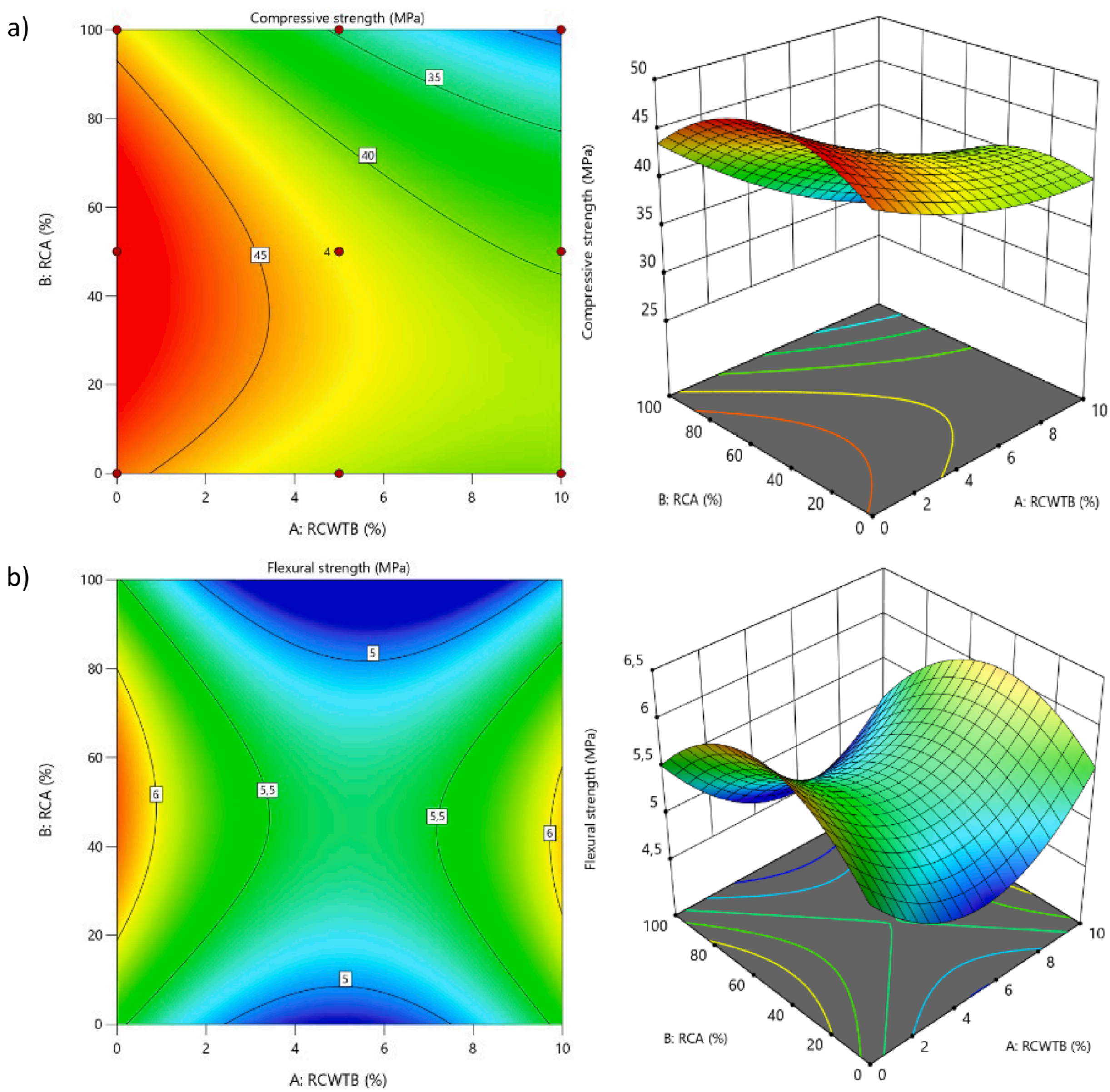

Fig. 9. Contour lines and 3D surfaces of quadratic models for $\alpha = \pm 1$: (a) compressive strength; (b) flexural strength.

Regarding compressive strength, it can be noted that lower strength values are associated with higher additions of RCWTB, mainly when combined with high amounts of coarse RCA, whereas the concave curvature of the surface indicates that higher values correspond to 50 % substitution of coarse aggregate with RCA. Regarding flexural strength, the results confirmed the literature reviewed [62,70] showing that increasing fiber content in concrete mixes leads to high flexural strength, as can be observed in the 3D graph in Fig. 9b. Furthermore, through its two curvatures, it accurately shows that high RCWTB additions resulted in increased flexural strength, especially when combined with RCA substitutions within intermediate range values, although a slight loss was noted for RCWTB contents of 5 %.

Finally, normal distribution plots were developed to compare the differences between the predicted and experimental values, as shown in Fig. 10. It was observed that, for each model, the points corresponding to the compressive strength and flexural strength values obtained from the tests consistently exhibited proximity to the fitted distribution lines in each case.

4.3. Multiple response optimization

One of the advantages of optimization is the simultaneous consideration of multiple responses to select the optimal combination of the concrete mix components [71]. This research focuses on the mechanical properties of concrete mixtures, specifically compressive strength and flexural strength, as they are usually the most relevant in concrete performance [72,73]. The interaction of RCWTB and RCA was analyzed for various goals related to these properties. Table 10 presents the predicted values obtained for four scenarios where the objective was to maximize/minimize each of the variables. Additionally, the desirability value was analyzed to evaluate the efficacy of each model. These scenarios allowed defining the suitability of the use of both wastes in several types of applications:

- In the scenario aiming to maximize both variables, compressive and flexural strength, a high desirability value was achieved (0.956), indicating a successful optimization process. RCA content was optimized to nearly 50 % substitution within the mix, while optimum RCWTB content was 0 %, indicating that the influence of RCA was highly significant for improving compressive strength values. Thus, the use of coarse RCA from a parent concrete with high strength can be adequate in structural elements in which high compressive and flexural strengths are required, such as long-span beams [74].
- The second scenario evaluated the opposite situation, aiming to obtain minimum required values of both properties. With a desirability value of 0.914, this ensured an effective optimization process. Both waste contents were found to be near the upper limits for each case, resulting in lower strengths, reflecting the impact of high percentages of RCWTB and RCA on reducing mechanical properties. Therefore, the simultaneous use of high contents of both residues is recommended when an optimal mechanical behavior is not required, for example in a blinding concrete [75,76].
- The scenario aiming to maximize compressive strength, regardless of the values obtained for flexural strength, simulates a situation, for example, of a column under pure compression [77,78]. This scenario provided a low RCWTB content of 3.76 % and 0 % substitution of NA by RCA. For this case, a desirability value below 0.90 was obtained.
- Finally, when maximizing flexural strength regardless of the value of compressive strength, an interesting situation for the design of concrete for pavements [79], the model obtained reflects the least optimal solution with a desirability value of 0.602. The % RCWTB

Table 10
Multi-objective optimization results and desirability analysis.

	Independent variable		Dependent variable		Desirability
	% RCWTB	% RCA	Compressive strength (MPa)	Flexural strength (MPa)	
Goal	In range	In range	Maximum	Maximum	**0.956**
Optimization result	0	49.41	49.62	6.27	
Goal	In range	In range	Minimum	Minimum	**0.914**
Optimization result	8.48	100	30.34	4.75	
Goal	In range	In range	Maximum	Minimum	**0.824**
Optimization result	3.76	0	42.18	4.85	
Goal	In range	In range	Minimum	Maximum	**0.602**
Optimization result	10	71.41	36.17	5.82	

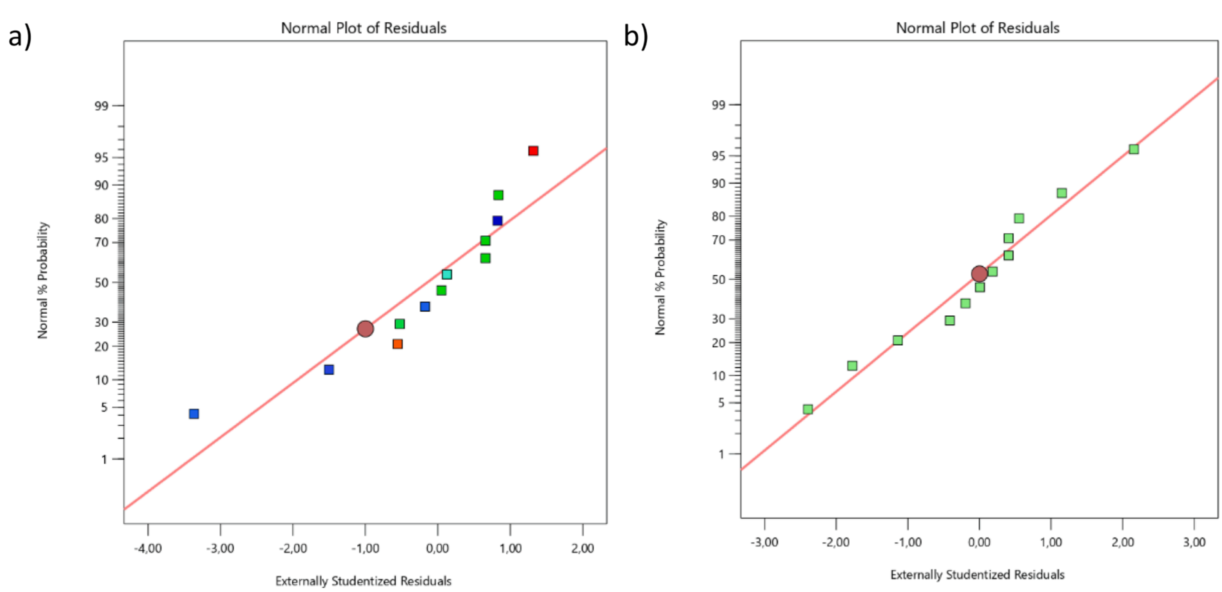

Fig. 10. Normal plots of the studentized residuals of quadratic models for α = ± 1: (a) compressive strength; (b) flexural strength.

was at the upper limit, thus benefiting the concrete from the stitching effect of the GFRP fibers, while the % RCA was at 71.41 %, resulting in moderate compressive strength and relatively high flexural strength.

In the pursuit of optimal combinations of both residues for their application in concrete elements, three cases based on strength ranges were rigorously evaluated through the use of overlay plots, as illustrated in Fig. 11. Initially, the objective was to maximize compressive strength at 28 days, aiming for values exceeding 45 MPa while ensuring that the flexural strength at 28 days remained within acceptable limits: this scenario was designated as Case Study I. In the second scenario, the optimization was carried out to maximize flexural strength, with target values above 5.5 MPa while maintaining compressive strength within acceptable bounds: this is referred to as Case Study II. Lastly, Case Study III aimed to simultaneously obtain suitable yet common values for compressive and flexural strength [34]. Thus, the value of the compressive strength was set between 30 MPa and 40 MPa, while a value higher than 5.0 MPa was established for the flexural strength. From the analysis of each case, several conclusions were drawn, along with their potential applications in structural elements.

- For Case Study I, the optimal region obtained concentrates combinations of both residues within an intermediate range for RCA and below 3 % for RCWTB. Combinations such as 1.11 % RCWTB and 12.54 % RCA result in concrete mixes reinforced with wind turbine blade fibers that could be suitable for application in columns. These structural elements have high demands in terms of compressive strength while not requiring stringent flexural strength [80]. Precast concrete applications, in which a compressive strength over 45 MPa is required, would also be an excellent target for the use of these mixtures [81].
- In Case Study II, the optimal region differed from Case Study I, with optimal combinations identified in two distinct areas of the graph. Optimal RCA values continued to be located in the intermediate zones, whereas successful combinations with RCWTB occurred below 3 % or above 7 %. This design could be ideal for applications in certain types of beams, which must ensure behavior under more rigorous flexural stresses than in the previous scenario [82], and well as for pavement applications [83].
- Combining requirements for both strengths, the final surface in Case Study III was obtained. Its region appeared to be much more restricted than previous ones, concentrated in the upper right part of the graph where RCA values were around 70 % replacement

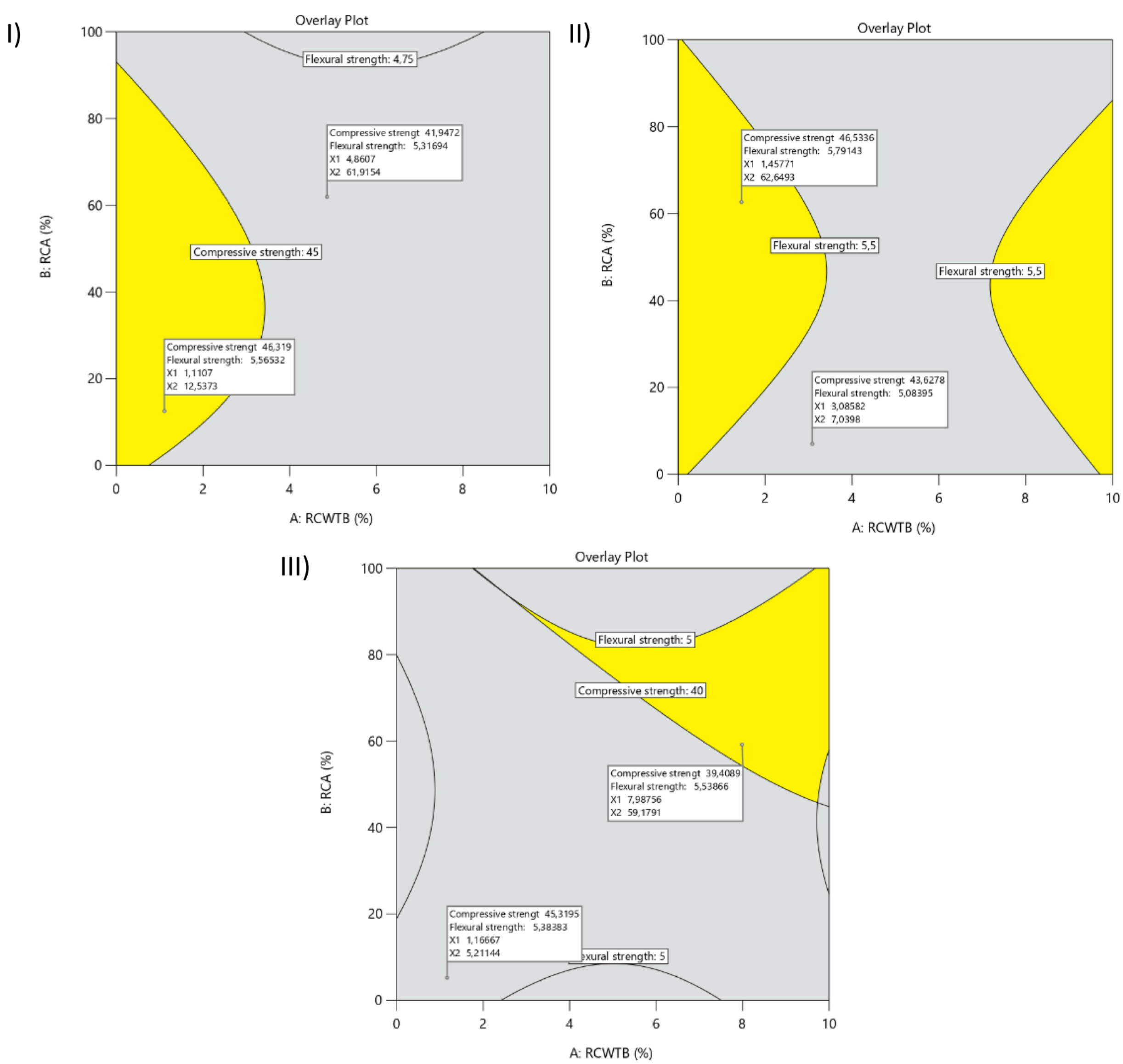

Fig. 11. Overlay plots showing optimal regions for each case study: (I), (II), (III).

alongside RCWTB values ranging between 6–10 %. Concrete for a wide variety of common applications could be designed with such waste combinations [84]. In addition, prefabricated elements such as slabs or panels, which have demanding compression requirements and need to withstand stresses during placement and construction [85], could also be executed with the mix combinations obtained in this surface [86].

All the values provided valuable insights into how different combinations of RCWTB and RCA impact mechanical properties, guiding the selection of customized material compositions for specific structural applications. Furthermore, the results from multi-objective optimization were aligned with those of the case studies, which provided robustness to the analysis, as well as a solid basis for defining the applicability of each combination of wastes.

5. Conclusions

In this study, the incorporation of RCA and RCWTB into concrete mixtures was examined, where RCA was used to replace coarse aggregate fractions at proportions ranging from 0 % to 100 %, while RCWTB was included as cement addition to the mixture at proportions ranging from 0 % to 10 % of the total mixture. The determination of the optimal combination of these two materials to produce concrete with specified mechanical properties was performed using an optimization tool based on the RSM. The following conclusions are drawn from this research:

1. Concrete mixtures incorporating RCA and RCWTB displayed modified fresh properties. Increasing RCA content reduced workability due to its high-water absorption, with the lowest slump values observed when combined with 10 % RCWTB. Fresh density values were marginally decreased owing to the lower density of the incorporated residues. Furthermore, the combined use of RCA and RCWTB increased the air content of the mixture, attributed to RCA's porosity and air retention of the RCWTB components.
2. All tested mixtures achieved the minimum compressive strength requirement of 25 MPa. Strength reductions were observed when increasing the residue content, averaging 1.80 MPa for every 50 % substitution of RCA, and more pronounced at up to 3.94 MPa for each 5 % inclusion of RCWTB. The overall compressive behavior was mainly linked to weak ITZ zones from the adhered mortar of the RCA and the reduced adhesion of RCWTB components to the cementitious matrix.
3. The addition of RCWTB to the mixtures improved flexural strength due to the presence of GFRP-composite fibers in the residue, which caused a stitching effect within the matrix. Increases of up to 14.67 % in flexural strength, as seen in the *W10RCA50* mixture, indicate the optimum interaction of the RCWTB with 50 % coarse RCA, as well as the beneficial properties of the incorporation of both materials into the concrete.
4. ANOVA analysis determined that quadratic regression models and the consideration of an α value of ± 1 in a central composite design provided a better fit to the experimental results of compressive and flexural strength. The R^2 values obtained for these models were high, reflecting enhanced predictive capability in the optimization process.
5. Multi-objective optimization facilitated the attainment of optimal combinations of both residues suitable for application in structural elements. For instance, the combination of intermediate values of RCA and low values of RCWTB ensured optimal compressive and flexural strengths. Notably, high RCWTB content also resulted in elevated flexural strength, particularly when combined with approximately 50 % RCA. This demonstrates the effectiveness of the combined use of these materials in structural elements, as well as in applications such as beams or pavements, where high flexural strength is essential.

It is concluded that the incorporation of RCWTB, combined with the replacement of coarse aggregates with RCA, significantly influenced the mechanical behavior of the designed concrete mixtures. The strength of the parent concrete and the stitching effect provided by the fibers from the RCWTB have proven critical factors for enhancing the strength of these concretes when evaluated at 28 days. However, it should be noted that these results have been obtained from RCA and RCWTB with specific characteristics, which may vary widely depending on their origin. In addition, the optimization has been conducted on the basis of results obtained with waste contents between two clearly defined limits and at a single age of concrete. Future research could address the analysis of the strength performance of concrete at other ages, with RCA and RCWTB from other origins and with other waste contents. A larger amount of experimental data, coupled with a deeper understanding of the physical behavior of concrete simultaneously containing RCA and RCWTB, would enable the optimization of its strength behavior through the use of mathematical and computational methods. Future research could also further investigate the impact of RCWTB and RCA on all the mechanical properties of concrete, with the goal of fully optimizing the mixtures from a holistic approach.

CRediT authorship contribution statement

Nerea Hurtado-Alonso: Writing – original draft, Validation, Software, Methodology, Investigation, Formal analysis, Conceptualization. **Javier Manso-Morato:** Visualization, Validation, Software, Methodology, Investigation, Formal analysis, Conceptualization. **Víctor Revilla-Cuesta:** Writing – review & editing, Visualization, Validation, Software, Methodology, Investigation, Formal analysis. **Marta Skaf:** Writing – review & editing, Supervision, Project administration, Methodology, Funding acquisition, Conceptualization.

Declaration of competing interest

The authors declare that they have no known competing financial interests or personal relationships that could have appeared to influence the work reported in this paper.

Acknowledgements

This research work was supported by the Spanish Ministry of Universities, MICINN, AEI, EU, ERDF and NextGenerationEU/PRTR [grant numbers PID2020-113837RB-I00; 10.13039/501100011033; TED2021-129715 B–I00; PID2023-146642OB-I00; FPU21/04364]; the Junta de Castilla y León (Regional Government) and ERDF [grant number UIC-231; BU033P23; BU066-22]; and, finally, the University of Burgos [grant number SUCONS, Y135. GI].

Appendix A. Supplementary data

Supplementary data to this article can be found online at https://doi.org/10.1016/j.compstruct.2025.118895.

Data availability

All the data generated during the research are available throughout the article and its supplementary material.

References

[1] Samaniego E, Anitescu C, Goswami S, Nguyen-Thanh VM, Guo H, Hamdia K, et al. An energy approach to the solution of partial differential equations in computational mechanics via machine learning: concepts, implementation and applications. Comput Methods Appl Mech Eng 2020;362:112790. https://doi.org/10.1016/J.CMA.2019.112790.

[2] Khuri AI, Mukhopadhyay S. Response surface methodology, WIREs. Comput Stat 2010;2:128–49. https://doi.org/10.1002/wics.73.

[3] Smucker BJ, Edwards DJ, Weese ML. Response surface models: to reduce or not to reduce? J Qual Technol 2021;53:197–216. https://doi.org/10.1080/00224065.2019.1705208.
[4] Tavakoli H, Barkdoll BD. Sustainability-based optimization algorithm. Int J Environ Sci Technol 2020;17:1537–50. https://doi.org/10.1007/s13762-019-02535-9.
[5] Sadollah A, Nasir M, Geem ZW. Sustainability and optimization: from conceptual fundamentals to applications. Sustainability (Switzerland) 2020;12:2027. https://doi.org/10.3390/su12052027.
[6] Sabrin R, Shahjalal M, Eema Bachu HA, Lutful Habib MM, Jerin T, Billah AM. Recycling of different industrial wastes as supplement of cement for sustainable production of mortar, Journal of Building. Engineering 2024;86:108765. https://doi.org/10.1016/J.JOBE.2024.108765.
[7] Monteiro PJM, Miller SA, Horvath A. Towards sustainable concrete. Nat Mater 2017;16:698–9. https://doi.org/10.1038/nmat4930.
[8] Benhelal E, Shamsaei E, Rashid MI. Challenges against CO2 abatement strategies in cement industry: a review. J Environ Sci 2021;104:84–101. https://doi.org/10.1016/J.JES.2020.11.020.
[9] Hossein AH, AzariJafari H, Khoshnazar R. The role of performance metrics in comparative LCA of concrete mixtures incorporating solid wastes: a critical review and guideline proposal. Waste Manag 2022;140:40–54. https://doi.org/10.1016/J.WASMAN.2022.01.010.
[10] Lothenbach B, Scrivener K, Hooton RD. Supplementary cementitious materials. Cem Concr Res 2011;41:1244–56. https://doi.org/10.1016/J.CEMCONRES.2010.12.001.
[11] Silva RV, de Brito J, Dhir RK. Use of recycled aggregates arising from construction and demolition waste in new construction applications. J Clean Prod 2019;236:117629. https://doi.org/10.1016/J.JCLEPRO.2019.117629.
[12] Li Z, Lu D, Gao X. Optimization of mixture proportions by statistical experimental design using response surface method - A review. J Build Eng 2021;36:102101. https://doi.org/10.1016/j.jobe.2020.102101.
[13] Hammoudi A, Moussaceb K, Belebchouche C, Dahmoune F. Comparison of artificial neural network (ANN) and response surface methodology (RSM) prediction in compressive strength of recycled concrete aggregates. Constr Build Mater 2019;209:425–36. https://doi.org/10.1016/j.conbuildmat.2019.03.119.
[14] Xuan DX, Houben LJM, Molenaar AAA, Shui ZH. Mixture optimization of cement treated demolition waste with recycled masonry and concrete. Mater Struct/Mater Constr 2012;45:143–51. https://doi.org/10.1617/s11527-011-9756-3.
[15] Chiranjeevi K, Kumar DH, Srinivasa AS, Ravi Shankar AU. Optimisation of recycled concrete aggregates for cement-treated bases by response surface method. Int J Pavement Eng 2023;24:2179051. https://doi.org/10.1080/10298436.2023.2179051.
[16] Luo X, Xing G, Qiao L, Miao P, Yu X, Ma K. Multi-objective optimization of the mix proportion for dune sand concrete based on response surface methodology. Constr Build Mater 2023;366:129928. https://doi.org/10.1016/j.conbuildmat.2022.129928.
[17] Ghafari E, Costa H, Júlio E. RSM-based model to predict the performance of self-compacting UHPC reinforced with hybrid steel micro-fibers. Constr Build Mater 2014;66:375–83. https://doi.org/10.1016/J.CONBUILDMAT.2014.05.064.
[18] Dashti J, Nematzadeh M. Compressive and direct tensile behavior of concrete containing Forta-Ferro fiber and calcium aluminate cement subjected to sulfuric acid attack with optimized design. Constr Build Mater 2020;253:118999. https://doi.org/10.1016/j.conbuildmat.2020.118999.
[19] Patil S, Bhaskar R, Xavier JR, Raja R. Experimental evaluation and statistical modeling of sustainable sisal fiber-reinforced fly ash-based lateritic concrete using response surface methodology. J Build Eng 2024;84:108498. https://doi.org/10.1016/J.JOBE.2024.108498.
[20] WindEurope, WE, 2023. Statistics for the European wind-energy sector, (n.d.). https://windeurope.org/.
[21] Tazi N, Kim J, Bouzidi Y, Chatelet E, Liu G. Waste and material flow analysis in the end-of-life wind energy system. Resour Conserv Recycl 2019;145:199–207. https://doi.org/10.1016/J.RESCONREC.2019.02.039.
[22] Joustra J, Flipsen B, Balkenende R. Structural reuse of wind turbine blades through segmentation. Composites, Part C: Open Access 2021;5:100137. https://doi.org/10.1016/J.JCOMC.2021.100137.
[23] Baturkin D, Hisseine OA, Masmoudi R, Tagnit-Hamou A, Massicotte L. Valorization of recycled FRP materials from wind turbine blades in concrete. Resour Conserv Recycl 2021;174:105807. https://doi.org/10.1016/J.RESCONREC.2021.105807.
[24] Revilla-Cuesta V, Skaf M, Ortega-López V, Manso JM. Raw-crushed wind-turbine blade: waste characterization and suitability for use in concrete production. Resour Conserv Recycl 2023;198:107160. https://doi.org/10.1016/J.RESCONREC.2023.107160.
[25] Revilla-Cuesta V, Faleschini F, Pellegrino C, Skaf M, Ortega-López V. Water transport and porosity trends of concrete containing integral additions of raw-crushed wind-turbine blade. Dev Built Environ 2024;17:100374. https://doi.org/10.1016/J.DIBE.2024.100374.
[26] Tota-Maharaj K, McMahon A. Resource and waste quantification scenarios for wind turbine decommissioning in the United Kingdom,. Waste Dispos Sustain Energy 2021;3:117–44. https://doi.org/10.1007/s42768-020-00057-6.
[27] Majhi RK, Nayak AN, Mukharjee BB. Development of sustainable concrete using recycled coarse aggregate and ground granulated blast furnace slag. Constr Build Mater 2018;159:417–30. https://doi.org/10.1016/j.conbuildmat.2017.10.118.
[28] Singh N, Singh A, Ankur N, Kumar P, Kumar M, Singh T. Reviewing the properties of recycled concrete aggregates and iron slag in concrete. J Build Eng 2022;60:105150. https://doi.org/10.1016/j.jobe.2022.105150.
[29] Limbachiya M, Meddah MS, Ouchagour Y. Use of recycled concrete aggregate in fly-ash concrete. Constr Build Mater 2012;27:439–49. https://doi.org/10.1016/J.CONBUILDMAT.2011.07.023.
[30] Silva S, Evangelista L, de Brito J. Durability and shrinkage performance of concrete made with coarse multi-recycled concrete aggregates. Constr Build Mater 2021;272:121645. https://doi.org/10.1016/J.CONBUILDMAT.2020.121645.
[31] Batikha M, Ali STM, Rostami A, Kurtayev M. Using recycled coarse aggregate and ceramic waste to produce sustainable economic concrete. Int J Sustain Eng 2021;14:785–99. https://doi.org/10.1080/19397038.2020.1862353.
[32] EN-Euronorm, European Comittee for Standardization, Rue de Stassart, 36. Belgium-1050 Burssels, 2020.
[33] Lee J, Lothenbach B, Moon J. Performance improvement of Portland-limestone cement by mechanochemical activation. Cem Concr Res 2024;176:107411. https://doi.org/10.1016/J.CEMCONRES.2023.107411.
[34] Eurocode 2, Design of Concrete Structures. Part 1-1: General Rules and Rules for Buildings (EN 1992-1-1), CEN (European Comittee for Standardization), 2010.
[35] Silva RV, de Brito J, Dhir RK. Fresh-state performance of recycled aggregate concrete: a review. Constr Build Mater 2018;178:19–31. https://doi.org/10.1016/J.CONBUILDMAT.2018.05.149.
[36] Revilla-Cuesta V, Manso-Morato J, Hurtado-Alonso N, Skaf M, Ortega-López V. Mechanical and environmental advantages of the revaluation of raw-crushed wind-turbine blades as a concrete component. J Build Eng 2024;82:108383. https://doi.org/10.1016/J.JOBE.2023.108383.
[37] Trento D, Faleschini F, Revilla-Cuesta V, Ortega-López V. Improving the early-age behavior of concrete containing coarse recycled aggregate with raw-crushed wind-turbine blade. J Build Eng 2024;92:109815. https://doi.org/10.1016/J.JOBE.2024.109815.
[38] Ortega-López V, Faleschini F, Hurtado-Alonso N, Manso-Morato J, Revilla-Cuesta V. Analysis of raw-crushed wind-turbine blade as an overall concrete addition: stress–strain and deflection performance effects. Compos Struct 2024;340:118170. https://doi.org/10.1016/J.COMPSTRUCT.2024.118170.
[39] Makul N, Fediuk R, Amran M, Zeyad AM, Murali G, Vatin N, et al. Use of recycled concrete aggregates in production of green cement-based concrete composites: a review. Crystals (Basel) 2021;11:232. https://doi.org/10.3390/cryst11030232.
[40] Kurda R, de Brito J, Silvestre JD. Influence of recycled aggregates and high contents of fly ash on concrete fresh properties. Cem Concr Compos 2017;84:198–213. https://doi.org/10.1016/J.CEMCONCOMP.2017.09.009.
[41] Wang W, Shen A, Lyu Z, He Z, Nguyen KTQ. Fresh and rheological characteristics of fiber reinforced concrete——A review. Constr Build Mater 2021;296:123734. https://doi.org/10.1016/J.CONBUILDMAT.2021.123734.
[42] Mahboob A, Hassanshahi O, Safi M, Majid TA. Experimental investigation of eco-friendly fiber-reinforced concrete using recycled and natural fibers, integrated with recycled aggregates. Adv Compos Mater 2024. https://doi.org/10.1080/09243046.2024.2322799.
[43] Poon CS, Shui ZH, Lam L, Fok H, Kou SC. Influence of moisture states of natural and recycled aggregates on the slump and compressive strength of concrete. Cem Concr Res 2004;34:31–6. https://doi.org/10.1016/S0008-8846(03)00186-8.
[44] Pacheco J, de Brito J, Chastre C, Evangelista L. Recycled concrete for structural applications. Recyc Concr Technol Perfor 2023:195–231. https://doi.org/10.1016/B978-0-323-85210-4.00011-4.
[45] Fu B, Xu GT, Sen Peng W, Huang JZ, Zou QQ, Y.. Di Kuang, Performance enhancement of recycled coarse aggregate concrete by incorporating with macro fibers processed from waste GFRP. Constr Build Mater 2024;411:134166. https://doi.org/10.1016/J.CONBUILDMAT.2023.134166.
[46] Lavado J, Bogas J, de Brito J, Hawreen A. Fresh properties of recycled aggregate concrete. Constr Build Mater 2020;233:117322. https://doi.org/10.1016/J.CONBUILDMAT.2019.117322.
[47] Bentegri I, Boukendakdji O, Kadri EH, Ngo TT, Soualhi H. Rheological and tribological behaviors of polypropylene fiber reinforced concrete. Constr Build Mater 2020;261:119962. https://doi.org/10.1016/J.CONBUILDMAT.2020.119962.
[48] Kazemian M, Shafei B. Mechanical properties of hybrid fiber-reinforced concretes made with low dosages of synthetic fibers. Struct Concr 2023;24:1226–43. https://doi.org/10.1002/suco.202100915.
[49] Yazdanbakhsh A, Bank LC, Rieder KA, Tian Y, Chen C. Concrete with discrete slender elements from mechanically recycled wind turbine blades. Resour Conserv Recycl 2018;128:11–21. https://doi.org/10.1016/J.RESCONREC.2017.08.005.
[50] Verian KP, Ashraf W, Cao Y. Properties of recycled concrete aggregate and their influence in new concrete production. Resour Conserv Recycl 2018;133:30–49. https://doi.org/10.1016/J.RESCONREC.2018.02.005.
[51] Jang E-S, Kang C-W. Porosity analysis of three types of balsa (Ochroma pyramidale) wood depending on density. J Wood Sci 2022;68:31. https://doi.org/10.1186/s10086-022-02037-2.
[52] Keun-Hyeok Yang H-S-C, Ashour AF. Influence of type and replacement level of recycled aggregates on concrete properties. ACI Mater J 2008;105:289–96. https://doi.org/10.14359/19826.
[53] Soares D, De Brito J, Ferreira J, Pacheco J. Use of coarse recycled aggregates from precast concrete rejects: mechanical and durability performance. Constr Build Mater 2014;71:263–72. https://doi.org/10.1016/J.CONBUILDMAT.2014.08.034.
[54] Silva RV, de Brito J, Dhir RK. The influence of the use of recycled aggregates on the compressive strength of concrete: a review. Eur J Environ Civ Eng 2015;19:825–49. https://doi.org/10.1080/19648189.2014.974831.
[55] Sérifou M, Sbartaï ZM, Yotte S, Boffoué MO, Emeruwa E, Bos F. A study of concrete made with fine and coarse aggregates recycled from fresh concrete waste. J Constr Eng 2013;2013:317182. https://doi.org/10.1155/2013/317182.

[56] Bao J, Li S, Zhang P, Ding X, Xue S, Cui Y, et al. Influence of the incorporation of recycled coarse aggregate on water absorption and chloride penetration into concrete. Constr Build Mater 2020;239:117845. https://doi.org/10.1016/J.CONBUILDMAT.2019.117845.

[57] Sasanipour H, Aslani F. Durability properties evaluation of self-compacting concrete prepared with waste fine and coarse recycled concrete aggregates. Constr Build Mater 2020;236:117540. https://doi.org/10.1016/J.CONBUILDMAT.2019.117540.

[58] Djerbi A. Effect of recycled coarse aggregate on the new interfacial transition zone concrete. Constr Build Mater 2018;190:1023–33. https://doi.org/10.1016/J.CONBUILDMAT.2018.09.180.

[59] Islam MJ, Shahjalal M, Haque NMA. Mechanical and durability properties of concrete with recycled polypropylene waste plastic as a partial replacement of coarse aggregate. J Build Eng 2022;54:104597. https://doi.org/10.1016/J.JOBE.2022.104597.

[60] Zhang H, Ji T, Liu H. Performance evolution of the interfacial transition zone (ITZ) in recycled aggregate concrete under external sulfate attacks and dry-wet cycling. Constr Build Mater 2019;229:116938. https://doi.org/10.1016/J.CONBUILDMAT.2019.116938.

[61] Xu F, Tian B, Xu G. Influence of the ITZ thickness on the damage performance of recycled concrete. Adv Mater Sci Eng 2021;2021:643956. https://doi.org/10.1155/2021/6643956.

[62] Balagopal V, Panicker AS, Arathy MS, Sandeep S, Pillai SK. Influence of fibers on the mechanical properties of cementitious composites - a review. Mater Today Proc 2022;65:1846–50. https://doi.org/10.1016/J.MATPR.2022.05.023.

[63] Bui NK, Satomi T, Takahashi H. Mechanical properties of concrete containing 100% treated coarse recycled concrete aggregate. Constr Build Mater 2018;163:496–507. https://doi.org/10.1016/J.CONBUILDMAT.2017.12.131.

[64] Otsuki N, Yodsudjai W, Nishida T, Yamane H. Developed method for measuring flexural strength and modulus of elasticity of micro-regions in normal and recycled aggregate concretes. Mag Concr Res 2003;55:439–48. https://doi.org/10.1680/macr.2003.55.5.439.

[65] Zhao Z, Liu Y, Lu Y, Ji C, Lin C, Yao L, et al. Prediction of properties of recycled aggregate concrete using machine learning models: a critical review. J Build Eng 2024;90:109516. https://doi.org/10.1016/J.JOBE.2024.109516.

[66] Gómez-Soberón JMV. Porosity of recycled concrete with substitution of recycled concrete aggregate: an experimental study. Cem Concr Res 2002;32:1301–11. https://doi.org/10.1016/S0008-8846(02)00795-0.

[67] Kim J, Jeong S, Kim H, Kim Y, Park S. Bond strength properties of GFRP and CFRP according to concrete strength. Appl Sci 2022;12:10611. https://doi.org/10.3390/app122010611.

[68] Bidabadi MS, Akbari M, Panahi O. Optimum mix design of recycled concrete based on the fresh and hardened properties of concrete. J Build Eng 2020;32:101483. https://doi.org/10.1016/J.JOBE.2020.101483.

[69] Chakradhara Rao M. Properties of recycled aggregate and recycled aggregate concrete: effect of parent concrete. Asian J Civ Eng 2018;19:103–10. https://doi.org/10.1007/s42107-018-0011-x.

[70] Sivakumar A, Santhanam M. Mechanical properties of high strength concrete reinforced with metallic and non-metallic fibres. Cem Concr Compos 2007;29:603–8. https://doi.org/10.1016/J.CEMCONCOMP.2007.03.006.

[71] Şimşek B, İç YT, Şimşek EH. A RSM-based multi-response optimization application for determining optimal mix proportions of standard ready-mixed concrete. Arab J Sci Eng 2016;41:1435–50. https://doi.org/10.1007/s13369-015-1987-0.

[72] Kovler K, Roussel N. Properties of fresh and hardened concrete. Cem Concr Res 2011;41:775–92. https://doi.org/10.1016/J.CEMCONRES.2011.03.009.

[73] Abbass W, Khan MI, Mourad S. Evaluation of mechanical properties of steel fiber reinforced concrete with different strengths of concrete. Constr Build Mater 2018;168:556–69. https://doi.org/10.1016/J.CONBUILDMAT.2018.02.164.

[74] Choi Y-C, Kim J-Y, Lee K-S, Jung J-S. Experimental study on structural performance of new steel-concrete composite beam for both long-span and low-height parking structures. J Asian Architect Build Eng 2023;22:1028–49. https://doi.org/10.1080/13467581.2022.2044822.

[75] Agarwal M, del Rey Castillo E. Normal and controlled low-strength material concrete with high volume of fly ash and glass waste. ACI Mater J 2022;119:75–88. https://doi.org/10.14359/51734687.

[76] Ibrahim M, Rahman MK, Najamuddin SK, Alhelal ZS, Acero CE. A review on utilization of industrial by-products in the production of controlled low strength materials and factors influencing the properties. Constr Build Mater 2022;325:126704. https://doi.org/10.1016/J.CONBUILDMAT.2022.126704.

[77] Lee T-K, Chen C-C, Pan ADE, Hsiue K-Y, Tsai W-M, Hwa K. Experimental evaluation of large circular RC columns under pure compression. Struct Concr 2013;14:60–8. https://doi.org/10.1002/suco.201200012.

[78] Uy B. Strength of concrete filled steel box columns incorporating local buckling. J Struct Eng (N Y N Y) 2000;126:341–52. https://doi.org/10.1061/(ASCE)0733-9445(2000)126:3(341).

[79] Pranav S, Aggarwal S, Yang EH, Kumar Sarkar A, Pratap Singh A, Lahoti M. Alternative materials for wearing course of concrete pavements: a critical review. Constr Build Mater 2020;236:117609. https://doi.org/10.1016/J.CONBUILDMAT.2019.117609.

[80] Cao Q, Jia J, Zhang L, Ye H, Lv X. Experimental study of axial compression of reinforced concrete columns made by environment-friendly post-filling coarse aggregate process. Struct Concr 2021;22:1671–87. https://doi.org/10.1002/suco.202000271.

[81] Martins R, do Carmo R, Costa H, Júlio E. Low cement concretes with ultra-high durability for innovative composite lightweight precast walls. J Build Eng 2024;86:108922. https://doi.org/10.1016/J.JOBE.2024.108922.

[82] Zhang Z, Leng J, Bian X, Xie T, Xu T. A refined model for the flexural behavior of reinforced UHPC members under sustained loading. J Build Eng 2024;93:109853. https://doi.org/10.1016/J.JOBE.2024.109853.

[83] Mansourian A, Shabani S, Siamardi K. Evaluation of fracture energy and durability properties of pavement concrete incorporating blends of durable and non-durable limestone Aggregates: RSM modelling and optimization. Theor Appl Fract Mech 2024;131:104374. https://doi.org/10.1016/J.TAFMEC.2024.104374.

[84] Yang Y, Lu P, Shao R, Zhao Q, Yang T, Wu C. A comprehensive review of multisource solid wastes in sustainable concrete: from material properties to engineering application. Constr Build Mater 2024;435:136775. https://doi.org/10.1016/J.CONBUILDMAT.2024.136775.

[85] Maya LF, Zanuy C, Albajar L, Lopez C, Portabella J. Experimental assessment of connections for precast concrete frames using ultra high performance fibre reinforced concrete. Constr Build Mater 2013;48:173–86. https://doi.org/10.1016/J.CONBUILDMAT.2013.07.002.

[86] Abdulrahman MB, Khazaal AS, Al-Attar AA, Dawood SH. Reinforced concrete slabs containing recycled concrete as coarse aggregate. In: Haido JH, Al-Sulaifanie BKM, Hassan LH, Jalil SA, Atroshey SMS, Saeed AF, Haleem DAJ, Adam SM, Al-Kamaki YSS, Hussain MS, Aswad NH, Mahmood NS, Mohammed NM, Ali IA, editors. IOP Conference Series: Materials Science and Engineering. IOP Publishing Ltd; 2020. https://doi.org/10.1088/1757-899X/978/1/012032.